JOURNAL OF GEOPHYSICAL RESEARCH, VOL. 112, D12S17, doi:10.1029/2006JD007925, 2007

A comparison of satellite tropospheric carbon monoxide measurements from AIRS and MOPITT during INTEX-A

Juying Warner,[1] M. McCourt Comer,[2] C. D. Barnet,[3] W. W. McMillan,[2] W. Wolf,[4] E. Maddy,[4] and G. Sachse[5]

Received 16 August 2006; revised 17 November 2006; accepted 28 February 2007; published 9 June 2007.

[1] Satellite CO measurements from Measurements of Pollution in the Troposphere (MOPITT) and Atmospheric Infrared Sounder (AIRS) were used in the Intercontinental Chemical Transport Experiment–North America (INTEX-A) by the flight planning team to monitor local emissions and the transport of polluted air masses. Because simultaneous measurements of tropospheric CO from both AIRS and MOPITT were used by different investigators during this experiment, a cross reference and comparison are necessary to understand these two data sets and their impacts to the scientific conclusions developed from them. The global CO mixing ratios at 500 mbar, as well as the CO total column amount, are compared between the two instruments for both direct comparison and the comparison using the same a priori profile for the period from 15 June to 14 August 2004. Also presented are the comparisons of the remotely sensed profiles by AIRS, MOPITT, and the in situ profiles collected by the DACOM. In summary, both sensors agree very well on the horizontal distributions of CO represented by the high correlation coefficients (0.7–0.98), and they agree on the CO concentrations to within an average of 10–15 ppbv. Over land, the CO variability is higher, and the correlations between the two data sets are relatively lower than over ocean; however, there is no evidence of a systematic bias. Over the oceans where the CO concentration is smaller in the lower atmosphere, AIRS-MOPITT show a positive bias of 15–20 ppbv and the details are presented.

Citation: Warner, J., M. M. Comer, C. D. Barnet, W. W. McMillan, W. Wolf, E. Maddy, and G. Sachse (2007), A comparison of satellite tropospheric carbon monoxide measurements from AIRS and MOPITT during INTEX-A, *J. Geophys. Res.*, *112*, D12S17, doi:10.1029/2006JD007925.

1. Introduction

[2] As a primary pollutant and key precursor to tropospheric ozone production [*Crutzen et al.*, 1979; *Jonquières and Marenco*, 1998; *Fishman and Balok*, 1999; *Logan et al.*, 1981; *Logan*, 1999] quantifying tropospheric carbon monoxide abundance is a key target of instruments of NASA's Earth Observing Systems (EOS) program, such as those from Measurements of Pollution in the Troposphere (MOPITT) on Terra [*Drummond*, 1989], from Atmospheric Infrared Sounder (AIRS) on Aqua [*Aumann et al.*, 2003], and from Tropospheric Emission Spectrometer (TES) on Aura [*Beer et al.*, 2001; *Beer*, 2006; *Bowman et al.*, 2002; *Clough et al.*, 1995; *Luo et al.*, 2002]. Building on the heritage of space-borne CO remote sensing from Measurements of Air Pollution from Satellite (MAPS) flown on board the space shuttle in 1981, 1984, and twice in 1994 [*Reichle et al.*, 1982; *Reichle and Connors*, 1999; *Connors et al.*, 1999], MOPITT, AIRS, and TES provide nearly global daily tropospheric CO maps of the Earth for the duration of their missions. Future missions such as IASI on EUMETSAT's METOP and possibly CrIS on NPOESS will provide CO products and extend the CO long-term record into the future. To ensure high-quality CO long-term records and bias-free data sets between the different instruments, a thorough understanding of the differences between each instrument is essential.

[3] The Intercontinental Chemical Transport Experiment–North America (INTEX-A) provided atmospheric chemistry measurements including CO, O_3, and others species significant to the atmosphere over polluted continental regions and in outflow regions. CO in situ measurements were collected coincident with both Terra and Aqua overpasses to facilitate satellite validation. Satellite CO measurements from MOPITT and AIRS were used by the flight planning team to monitor local emissions and the transport of polluted air masses. Because simultaneous measurements of tropospheric CO from both AIRS and

[1]Joint Center for Earth Systems Technology, University of Maryland Baltimore County, Baltimore, Maryland, USA.
[2]Department of Physics, University of Maryland Baltimore County, Baltimore, Maryland, USA.
[3]Center for Satellite Applications and Research, National Environmental Satellite, Data and Information Service, NOAA, Camp Springs, Maryland, USA.
[4]QSS Group, Inc., Lanham, Maryland, USA.
[5]NASA Langley Research Center, Hampton, Virginia, USA.

0148-0227/07/2006JD007925$09.00

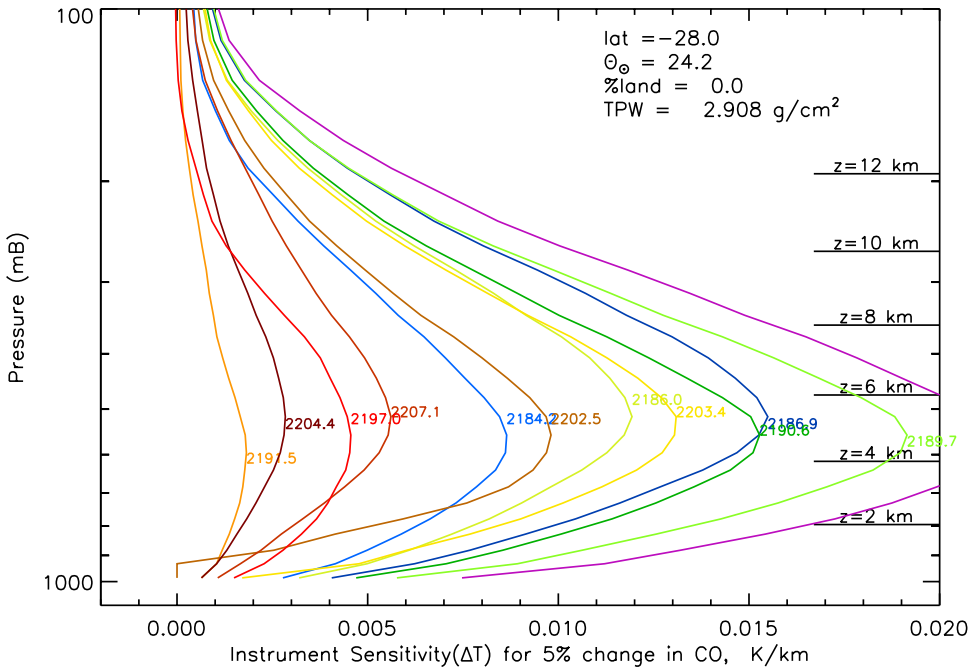

Figure 1. AIRS CO vertical sampling functions for selected channels in terms of brightness temperature changes for a 5% CO (p) perturbation of 1 km width for a midlatitude atmosphere.

MOPITT were used by different investigators during this experiment, a cross reference and comparison are necessary to understand these two data sets and their impacts to the scientific conclusions developed from them.

[4] This study is based on CO retrievals from a research version of the current AIRS operational physical algorithm and is compared to MOPITT CO retrievals employing a maximum a posteriori method [*Rodgers*, 2000]. The global CO mixing ratios at 500 mbar, as well as the CO total column amount, are compared between the two instruments. Also presented are the comparisons of vertical profiles that are measured by AIRS, MOPITT, and in situ by Differential Absorption CO Measurement (DACOM) [*Sachse et al.*, 1987]. Proper comparisons between two remote sensing instruments require the understanding of the contributions from the a priori information that is described by the averaging kernel [*Rodgers and Connor*, 2003]. This paper emphasizes the impact of the AIRS' first guess and averaging kernel to the intercomparisons with MOPITT without an attempt to optimize the AIRS CO retrieval algorithm.

2. Algorithms and Data

[5] As the first EOS sensor to observe tropospheric CO, MOPITT on board Terra was launched December 1999 and measures terrestrial thermal emission at 4.7 μm in the CO fundamental band using Correlation Radiometry [*Drummond*, 1989]. CO retrievals are obtained by using maximum a posteriori method that incorporates a priori information of the physical and statistical variability of the trace gas distribution in the atmosphere to choose the best solution. The trace gas variability is expressed in the form of the a priori vertical profile and covariance matrix that are compiled from a large number of in situ profiles taken over many years over the globe [*Pan et al.*, 1998; *Deeter et al.*, 2003]. The latest version, V3, uses a hybrid cloud detection method that incorporates the MODIS cloud mask with MOPITT radiances [*Warner et al.*, 2001]. *Emmons et al.* [2004], conducted the MOPITT validation against CMDL in situ profiles and concluded that MOPITT can measure atmospheric CO to an accuracy of within 20 ppbv at all levels, with higher agreements in the free atmosphere. Recent MOPITT validation studies using summer 2004 aircraft measurements by *Emmons et al.* [2007] show an agreement between MOPITT and DACOM/DC-8 to within 20 ppbv, and slightly larger differences for the COBRA-2004 and MOZAIC experiments.

[6] AIRS was launched on 4 May 2002 on board Aqua with the primary goals of providing accurate vertical profiles of temperature and water vapor in the Earth's atmosphere [*Aumann et al.*, 2003; *Susskind et al.*, 2003]. AIRS CO retrievals are obtained at 4.7 μm on the edge of the 1–0 vibration-rotation band of CO [*McMillan et al.*, 2005]. The instrument sensitivity functions for several AIRS CO channels are shown in Figure 1 indicating main sensitivity to midtropospheric CO between approximately 300 and 600 mbar. A research version of the AIRS science team retrieval codes, provided by coauthor Barnet, are used to retrieve atmospheric and surface physical parameters from AIRS spectra including temperature, water vapor, ozone, and CO [*Susskind et al.*, 2003].

[7] The current AIRS physical retrieval algorithm seeks to minimize the weighted difference between the clear column radiance observations and the radiance computed using a forward model [*Strow et al.*, 2003] by varying the geophysical state [*Susskind et al.*, 2003]. Furthermore, the changes to a group of the geophysical state are represented by a geophysical perturbation parameter and a perturbation function with trapezoidal shapes. Eigenvector decomposition technique is employed in the algorithm to solve for the

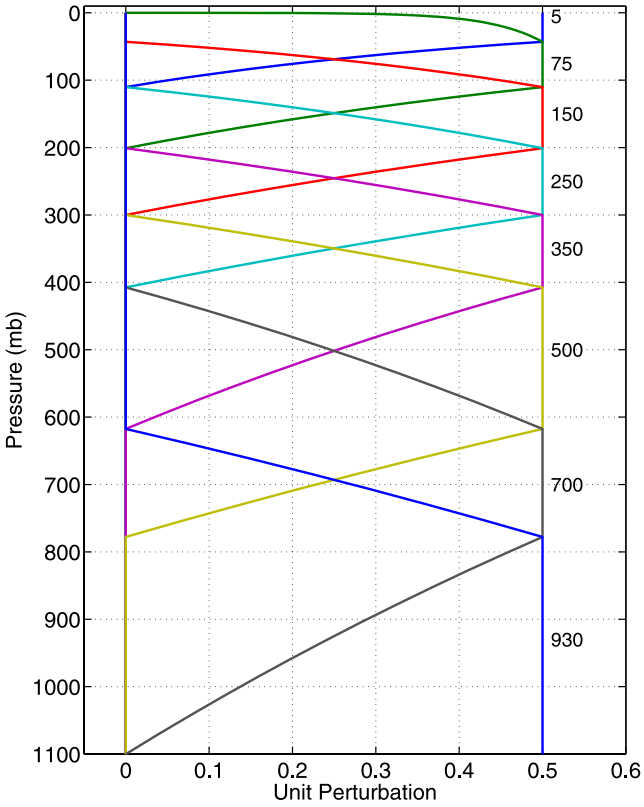

Figure 2. Trapezoidal functions used as oscillators in the AIRS science team algorithm, which was optimized to match the MOPITT vertical levels.

geophysical state, and a damping process is used to stabilize the solution [*Susskind et al.*, 2003]. The selection of the number and levels of the trapezoidal functions, the constraint magnitude for damping, and the choice of the first guess profile all affect the performance of the retrieval. *Comer* [2006] conducted the refinement study of this algorithm to suit the CO retrievals, which defines the optimal choice of these parameters. The present study employs one set of these parameters to best facilitate intercomparison with MOPITT. The trapezoidal functions used in this study were optimized to match the MOPITT vertical levels as illustrated by the effective pressure levels in Figure 2. The relevant forward model levels for these trapezoidal functions are also shown. The 32 spectral channels used to produce the data sets in this study are listed in the following subset of 52 channels in the CO region selected using principle component analysis: 2181.49, 2182.40, 2183.31, 2184.21, 2185.12, 2186.03, 2186.94, 2187.85, 2188.76, 2189.67, 2190.58, 2191.50, 2192.41, 2193.33, 2194.24, 2195.16, 2196.07, 2196.99, 2197.91, 2198.83, 2199.75, 2200.67, 2201.59, 2202.51, 2203.44, 2204.36, 2205.29, 2206.21, 2207.14, 2208.99, 2212.71, 2213.64, 2214.57, 2215.50, 2216.44, and 2221.12. The damping parameter $\Delta\lambda_{\text{critical}}$ [*Susskind et al.*, 2003] is given as 0.33 for this study. Because of the lack of observational sensitivity, an appreciable amount of the first guess profile often is retained in AIRS CO. This first guess profile is analogous to the a priori profile in the maximum a posteriori algorithm. During the field portion of INTEX-A, we used the AFGL standard atmosphere profiles [*Anderson et al.*, 1986] as the first guess to AIRS CO products for INTEX-A. We include AFGL first guess retrievals in the direct comparison portion of this study. However, we also present here AIRS CO retrievals using the MOPITT a priori as the AIRS first guess to minimize the differences introduced by the a priori for comparison purposes.

[8] On the basis of *Rodgers and Connor* [2003], an estimated profile from a retrieval algorithm is represented as the combination of a true profile and an a priori profile through the knowledge of an averaging kernel. The AIRS averaging kernel, shown as the A matrix in equation (1), indicates the sensitivity of the measurements to the CO concentrations at the retrieval levels defined by the trapezoids [*Susskind et al.*, 2003]. The details of the derivation and application of the averaging kernels will be discussed by coauthor Maddy in a separate paper, and the procedures used in this study are summarized below. The AIRS averaging kernel can be expressed as

$$A = U\frac{\lambda}{\lambda+\Delta\lambda}U^T, \tag{1}$$

where the matrix U are the eigenvectors from the unitary transformation, and λ are the eigenvalues of the eigenvectors damped by $\Delta\lambda$ as described by *Susskind et al.* [2003]. A is a (n $\times$ n) matrix where n is determined by the number of trapezoidal functions and, each row of matrix A represents the averaging kernel for the respective trapezoidal function. The convolution of the DACOM in situ profiles discussed in section 3.2 uses the following formula:

$$x' = x_0\left[1 + A\left(\frac{x - x_0}{x_0}\right)\right], \tag{2}$$

where x' represents the transformed in situ profile, x is the true profile, and x_0 is the a priori profile. Equation (2) is used in conjunction with equation (1) to convolve the in situ DACOM profiles in the comparison with AIRS retrievals.

[9] Two steps are taken to reduce the differences in the comparison of two instruments that are due to the influence of the a priori in the retrievals. First, we reprocessed the global data sets for the period of INTEX-A to use the MOPITT a priori as AIRS first guess. Thus the influence of the a priori retained in the retrievals are partially canceled. As a second step, we convolve the averaged AIRS retrievals using the MOPITT averaging kernels to simulate AIRS profiles seen in the MOPITT retrieval space to further demonstrate the agreement between the two sensors with minimized uncertainties introduced by the retrieval algorithm. Similar process can be repeated to convolve the average MOPITT profiles to the AIRS space using the AIRS averaging kernels, not shown here. The results of each approach are summarized in sections 3.2 and 3.3.

[10] The comparisons presented are from the INTEX-A experiment period of 15 June to 14 August 2004. The differences of the observation times between MOPITT and AIRS are generally a few hours since Terra is on an ascending orbit with an equator crossing time of 1030 local

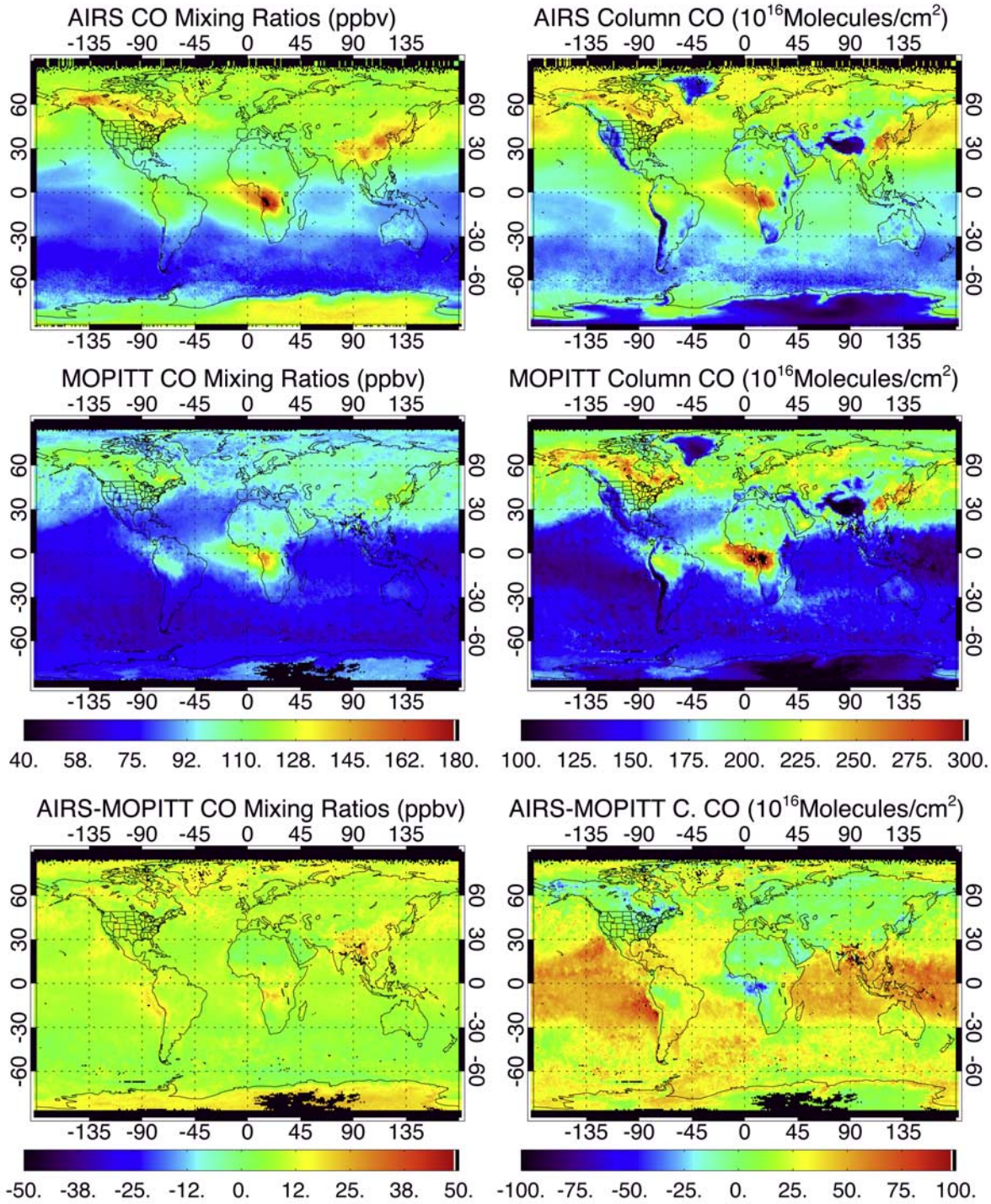

Figure 3. Global AIRS, MOPITT, and difference (AIRS-MOPITT) (left) CO total column maps and (right) 500 mbar mixing ratio maps, respectively, averaged over the period of 15 June to 14 August 2004.

time (LT) and Aqua is on a descending orbit with an equator crossing time of 1330 LT. The time difference is not a critical issue for the global comparisons of the data sets since we compare the averaged values for the 2-month period of INTEX-A. Although, the fact that AIRS and MOPITT do not see the same places on the same days could lead to some differences not accounted for by the different retrieval techniques. The time differences for the profile comparisons are discussed in detail in section 3.2. AIRS collects data at a spatial resolution of 13.5 km, however, the CO products are computed at approximately 45 km footprints as a result of the cloud clearing process

[*Susskind et al.*, 2003]. MOPITT collects data at a spatial resolution of 22 × 22 km at nadir providing higher CO spatial variability in comparison to the AIRS products. AIRS swaths, on the other hand, are approximately two and a half times wider than MOPITT swaths. For the comparisons of the globally averaged measurements over the 2-month period, the differing spatial resolutions do not impact the conclusions as much as they do the profile comparisons.

[11] Satellite global coverage also depends on the treatment of clouds, and since AIRS uses reconstructed cloudy pixels [*Susskind et al.*, 2003] while MOPITT removes cloudy pixels [*Warner et al.*, 2001], AIRS' horizontal data coverage is significantly higher. For the correlation studies, AIRS retrievals are screened additionally for clouds for this comparison work and only those pixels identified as less than 5% cloudy before cloud clearing are used to match the performance of MOPITT cloud detection algorithm which allows cloud coverage up to 5% and retrievals above low-level clouds.

3. Results and Discussions

3.1. Direct Comparison of Global Tropospheric CO

[12] AIRS and MOPITT CO mixing ratios at 500 hPa as well as the total column amounts are averaged over the INTEX-A period and for each 1 by 1° latitude and longitude. The selection of the binning area is based on the spatial resolutions of AIRS and MOPITT so that there are at least 4 pixels for AIRS in each area when cloud-cleared radiances are available. Figure 3 shows, on the left side, the global maps for the CO mixing ratios at 500 hPa for AIRS (top), MOPITT (middle), and the differences (AIRS-MOPITT, bottom), respectively. Similarly, the CO total column densities are shown in Figure 3 (right). The global CO mixing ratio differences at 500 hPa show apparent biases with AIRS higher than MOPITT by 10–20 ppbv over most areas. The differences are larger for higher CO plumes over the regions of biomass emissions, such as over Alaska and Canada during intensive fires [*Pfister et al.*, 2005] as well as over the African continent, and smaller for clean regions over the southern hemisphere oceans. The large differences over the Antarctic are most likely due to algorithm uncertainties over cold surfaces.

[13] The AIRS-MOPITT total column CO differences are larger, in a range of $25-75 \times 10^{16}$ molecules/cm^2, at low latitudes over ocean when the total column CO amounts are very low ($\sim 120 \times 10^{16}$ molecules/cm^2 from MOPITT). However, AIRS CO is smaller than MOPITT CO over northern hemisphere land when the total column CO amount is relatively high. This pattern of differences is in part due to the lack of measurement sensitivity in the lower atmosphere for down-looking spectrometers such as AIRS. The retrieved CO concentrations at these levels are heavily weighted by the first guess, and therefore proper first guess information in the retrieval algorithm is critical.

[14] The averaged CO mixing ratios at 500 hPa in the 1 × 1 grids are correlated and shown on Figure 4 for daytime land (top left), daytime ocean (top right), nighttime land (bottom left), and nighttime ocean (bottom right) respectively. Also shown are the histograms of the differences between AIRS and MOPITT averaged in the same fashion, indicating an average of 15 ppbv bias over all conditions. AIRS and MOPITT CO mixing ratios are very well correlated with the correlation coefficients at approximately 0.9 over ocean for both daytime and nighttime, and 0.84 for daytime land and 0.75 for nighttime land. These high correlation coefficients indicate that both sensors can capture the CO features with a good agreement. However, AIRS is consistently higher than MOPITT under all four conditions except for a small number of averaged grids with very low CO mixing ratios over the ocean. Daytime CO over land shows the highest variability, and over the oceans, the variability is much lower.

[15] With further inspection, one can note that in each panel in Figure 4 there are approximately two groups of data representing high and low CO. These two groupings appear as a bending in the data at approximately 100 ppbv for the ocean cases and are not well correlated. In the case of Night Land the scatterplots of the two data groups are merged in a way that misleads one to believe that for a narrow range of AIRS CO variation (100–110 ppbv) the MOPITT varies more than twice as much (70–110 ppbv). These high and low CO groups can be separated by analyzing the correlations for the northern and southern hemispheres independently, not shown here, since in the months of June to August the CO is much higher in the northern hemisphere than in the southern hemisphere as shown in Figure 3. This change in the correlation between high and low CO can be explained largely by the two different a priori profiles used in these retrievals for the two sensors since the AFGL profile is larger than the MOPITT a priori by approximately 20–30 ppbv between the surface and 500 hPa. This will also become evident when the same a priori is used for both sensors in the comparison discussions in section 3.3.

[16] Asymmetric probability distribution function (PDF) is evident in Figure 4 (top left) for the AIRS-MOPITT mixing ratios at 500 hPa for Day Land case, while non-Gaussian behavior is seen in the ocean, upper and lower right, and night land, lower left, cases. In the case of Day Land, the lower values can be fitted very well with Gaussian function representing larger variability in the background CO distributions due to a number of geophysical properties unique to the daytime land conditions that affect the retrievals such as the thermal contrasts, variations of the surface emissivity, possible cloud contaminations, etc. In contrast, over the ocean and nighttime land, the histograms show less variability in the CO mixing ratio differences between AIRS and MOPITT. There is a relatively small number of high values in the tail of the histogram in the Day Land case creating an asymmetric PDF representing a separate group of air masses that most likely originated from the biomass burning regions [*Sparling*, 2000].

3.2. Comparisons With INTEX-A in Situ Profiles

[17] During INTEX-A the DACOM instrument [*Sachse et al.*, 1987] was on board the NASA DC-8 and provided several in situ CO profiles coincident with the satellite overpasses [*Singh et al.*, 2006]. Three of which, 15 July, 2 August, and 7 August, are selected for this study. The location and sample sizes of each profile is summarized on the figure, and the binning sizes for all three cases are 4 × 4° of latitude and longitude from the centers of the spiral profiles. The 15 July profile was collected over Wisconsin

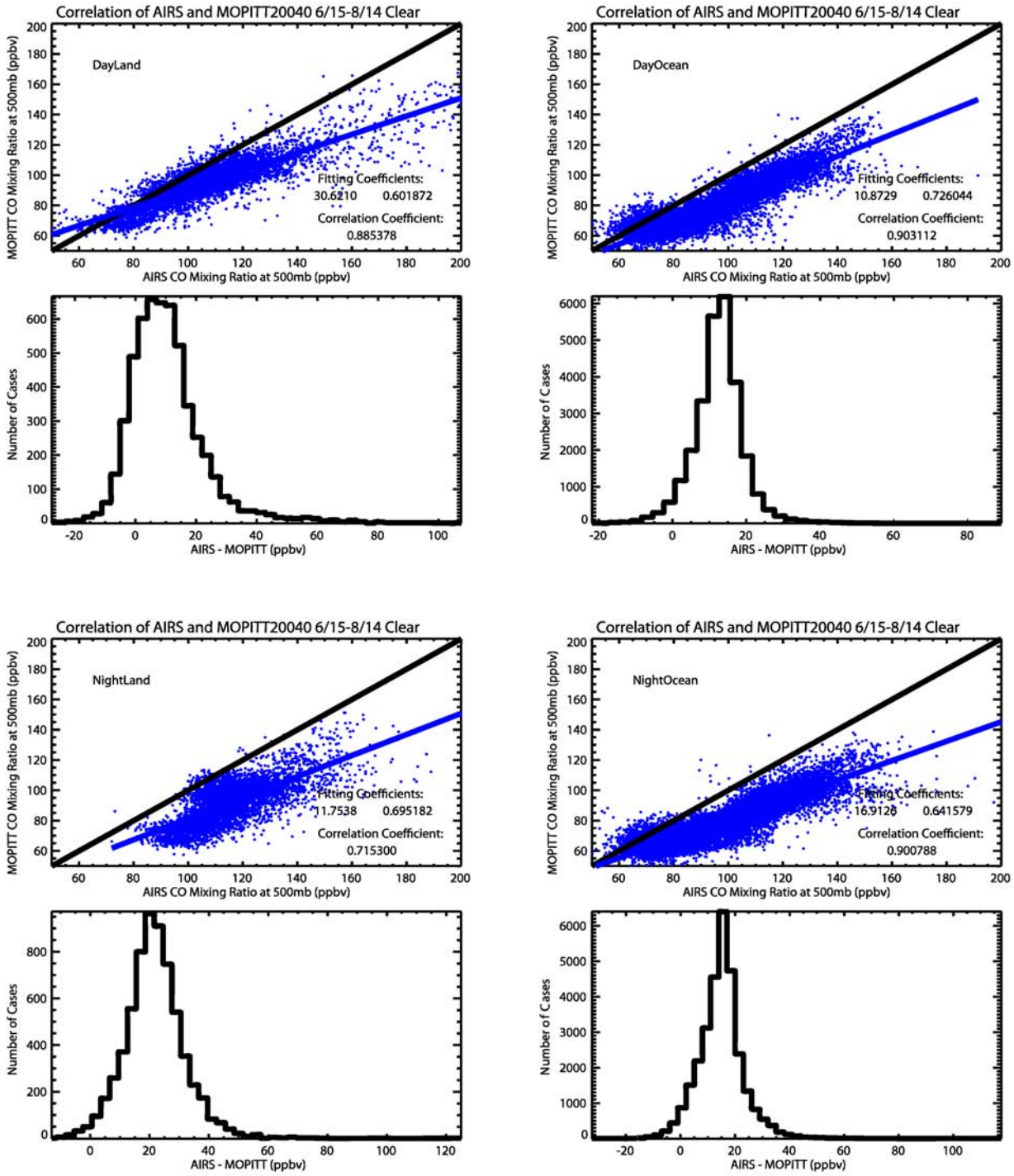

Figure 4. Correlated AIRS and MOPITT CO mixing ratios at 500 mbar averaged over INTEX-A period and for each 1 by 1° latitude and longitude for (top left) daytime land, (top right) daytime ocean, (bottom left) nighttime land, and (bottom right) nighttime ocean.

near the South shore of Lake Superior as shown in Figure 5. The vertical air column is relatively clean above 850 hPa and the CO peak below 850 hPa in DACOM is likely due to the combination of local emissions and the beginning of the transported fire emissions [*Pfister et al.*, 2005]. The spiral profile was collected starting at 1400 UT and lasted for 40 min while the AIRS overpass was at near 1900 UT, and MOPITT was at 1700 UT, all within a period of 5 hours. The 2 August DACOM was collected off the coast of Quebec, Canada over the Gulf of St Lawrence in the transported plumes of the fires indicated by high concentrations of CO in the layer from 550 to 800 hPa. The three sets of profiles, AIRS, MOPITT, and DACOM, were collected within a 2-hour period. Similarly, the 7 August

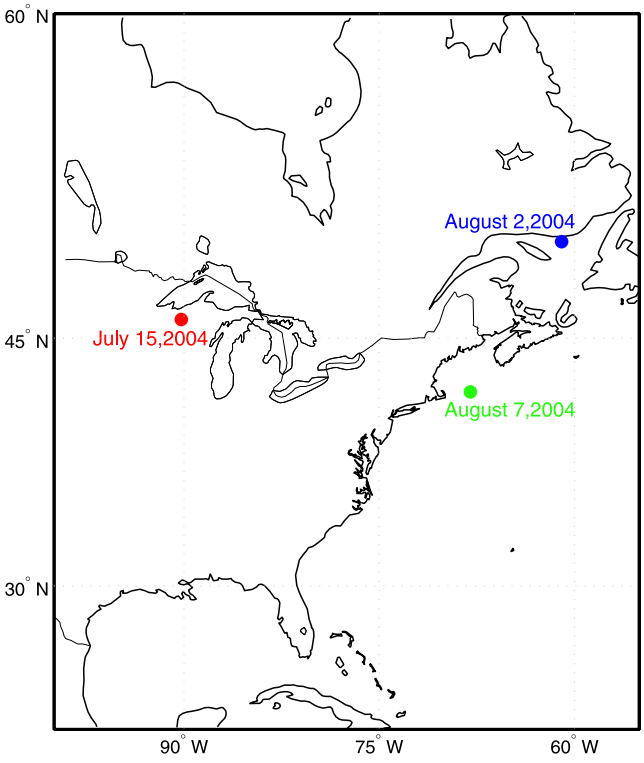

Figure 5. Northeast regional map showing the three locations of the DACOM profiles during INTEX-NA.

profile was collected off the coast of Massachusetts over the Atlantic Ocean in the air masses transported from North America and the data were collected within a period of less than 5 hours. The CO was better mixed vertically compared to the previous two profiles representing an older air mass with transported CO entrained into the lower atmosphere.

[18] Figure 6 shows the AIRS and MOPITT CO retrievals validated against the DACOM CO profiles for the dates of 15 July, 2 August, and 7 August 2004, respectively. The first two columns show the averaged, within 200 km of the spiral center point, AIRS CO mixing ratio profiles (red), MOPITT profiles (green), DACOM (blue), and AIRS first guess profiles (black). The MOPITT a priori is shown in the first column (in black) and the AFGL CO profile is shown in the second column (in black). The solid lines for AIRS and MOPITT are the averaged values and the dotted lines are the average ±SDV (Standard Deviations). The third column shows the average of the differences between the retrieved profiles and the transformed in situ DACOM profiles, for MOPITT (green) and AIRS (red). The fourth column is the DACOM profiles transformed to MOPITT retrieval (blue dashed) and the averaged AIRS profiles convolved to MOPITT retrieval (red dashed), as well as the mean MOPITT profile (green solid) and the mean AIRS profile (red solid). This practice can be carried out similarly by convolving the MOPITT profiles to the AIRS retrieval space as pointed out in the introduction.

[19] Over all, the three profiles agree within the range of data variability especially in the upper troposphere (250–550 hPa). The range of variation is larger for MOPITT than AIRS partly because there are more MOPITT data points in each 200 km radius area as a result of higher spatial resolution. Additionally, for the cases of 2 and 7 August, AIRS paths only cover part of the binning areas. The information content for MOPITT is generally 1.5 in the vertical, one piece of information is in the upper troposphere (250–350 hPa) and less than one in the lower troposphere at approximately 700 hPa [*Deeter et al.*, 2004]. AIRS CO channels are most sensitive in the upper and mid troposphere (300–600 hPa) and typically with less than one piece of information. The AIRS current CO retrieval algorithm clearly moves the first guess profile toward the observation where AIRS instrument is most sensitive, but it largely preserves the shape of the initial guess and thus has difficulty reproducing the DACOM revealed atmospheric structure. Both satellite observed profiles agree with DACOM at high and midtroposphere, but under estimate (for 15 July) or over estimate (for 2 August) in the lower atmosphere when there is little observation sensitivity especially when the air is very clean near the surface, i.e., 2 August 2004.

[20] Also important to note is that the tropospheric trace gas retrievals are largely dependent on the first guess profile even in the layers where the instruments are sensitive [*Rodgers*, 2000]. We have tested the AIRS CO retrieval using two different first guess profiles: one is from the AFGL standard atmosphere, which was used for the INTEX-A experiment and shown in the second column in Figure 6, and the other is using the MOPITT a priori profile shown in the first column of Figure 6. The AFGL profile is significantly higher (~30 ppbv) than the MOPITT a priori profile in the upper and lower troposphere, and the AIRS retrieval tends to converge too quickly resulting in a larger weighting from the first guess. This may have been due to the over constraint of the retrieval in an attempt to avoid the introduction of noise. For example, on 15 July, the AIRS retrieval reflects the observed CO in the layer of 300–500 hPa when the AFGL first guess is used, and reflects the CO layer below 500 hPa when the MOPITT a priori is used. A similar conclusion can be drawn from the 2 and 7 August profiles. The two retrievals agree better in the free troposphere when MOPITT a priori is used as the AIRS' first guess. This is not necessarily true in the lower troposphere since the instrument sensitivities are very different between the two sensors.

[21] As discussed in section 2, the retrieved profiles represent combinations of the a priori information and the true observations. To accurately compare the in situ profiles with the retrievals, the in situ profiles need to be convolved with the same sensitivity information used in the retrieval by using the averaging kernels from the retrieval outputs. The averaged differences between the convolved DACOM profiles and the retrieved MOPITT profiles are shown in the third column in green dashed lines for 15 July, 2 August, and 7 August 2004, respectively. Two of the three convolved in situ profiles agree extremely well with the MOPITT retrievals, the 7 August profile differs between the convolved in situ and the retrievals by up to 20 ppbv in the lower troposphere. DACOM profiles are also convolved with the AIRS equivalent averaging kernels (the A matrix) and the differences are shown as the dashed red lines in the third column for the three INTEX-NA profiles. The differences are larger than those from MOPITT in the midtropo-

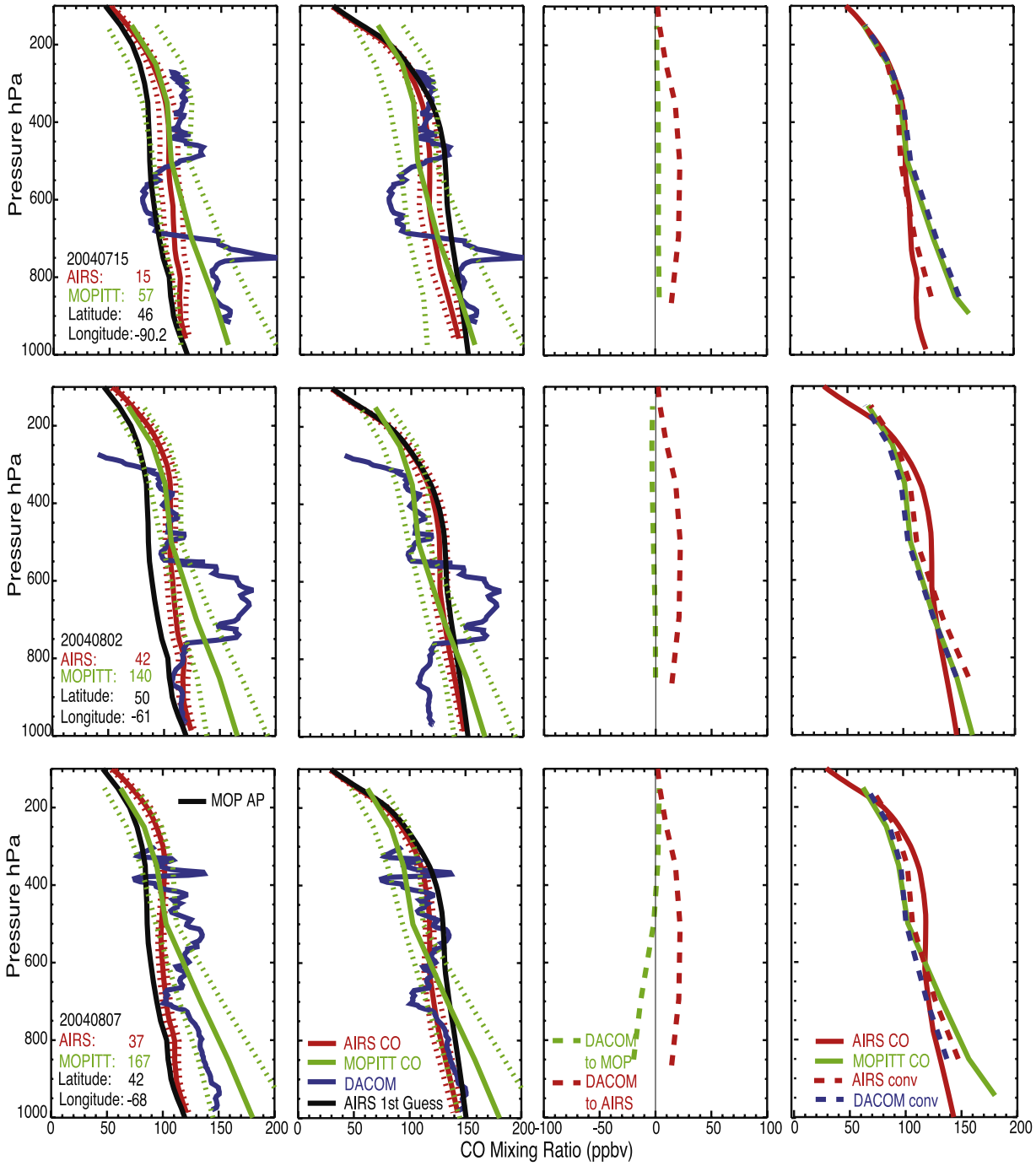

Figure 6. AIRS and MOPITT CO profiles validated against DACOM CO during INTEX-NA for the days of 15 July, 2 August, and 7 August 2004. The first two columns are the averaged, within approximately 200 km of the spiral point, AIRS CO mixing ratios profiles (red), MOPITT profiles (green), DACOM (blue), and the MOPITT a priori (for the first column) or AFGL CO profile (for the second column) as first guess profile for AIRS (black). The solid lines for AIRS and MOPITT are the averaged values and the dotted lines are the average ± SDV. The third column shows the average of the differences between the retrieved profiles and the convolved in situ DACOM profiles, to MOPITT (green) and to AIRS (red). The third column shows the convolved average AIRS profile (dashed red) and convolved DACOM profile (dashed blue) by MOPITT averaging kernel.

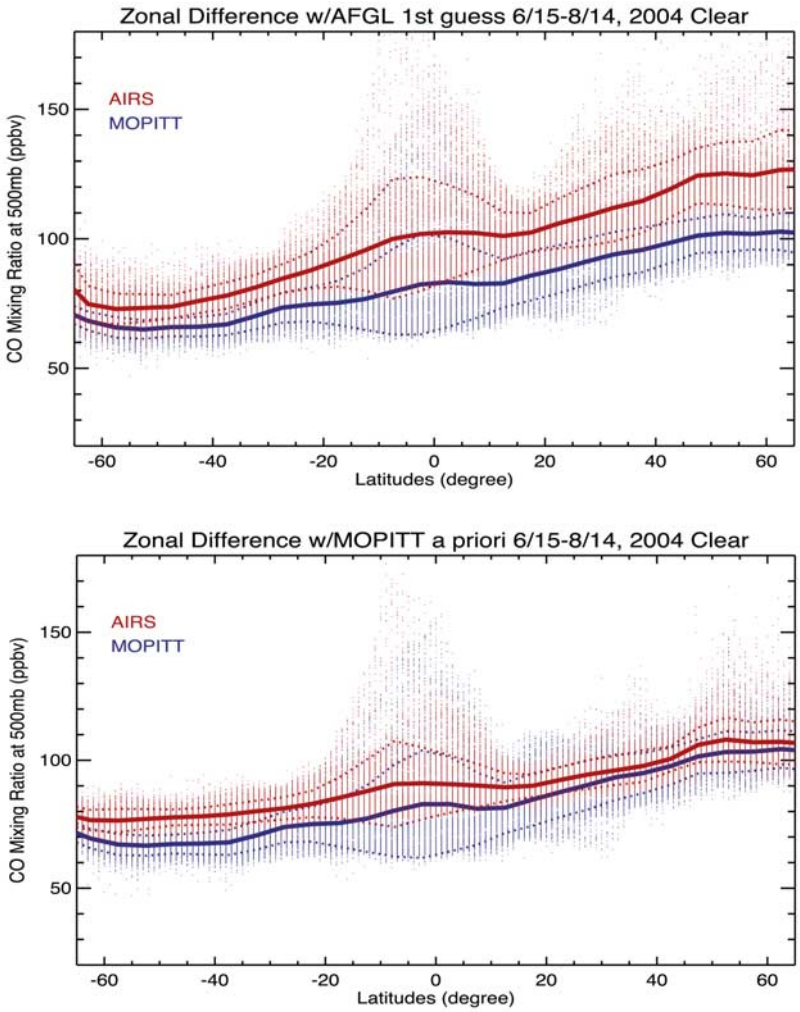

Figure 7. Comparison of zonal averaged CO mixing ratios at 500 mbar between AIRS (red) and MOPITT (blue). (top) Comparison when AIRS CO is retrieved using the AFGL first guess and (bottom) comparison when the MOPITT a priori is used as the first guess for AIRS for the period of 15 June to 14 August 2004. Scatterplots are the CO mixing ratios binned in $1 \times 1^{\circ}$ latitude and longitude boxes, solid curves are the zonal averages, and the dashed lines mark the ranges of the standard deviations.

sphere, up to 20 ppbv and appear to be more systematic. These differences are under investigation by the AIRS team.

[22] Profiles adjusted to the same a priori will partially offset the differences between MOPITT and AIRS retrievals; however, because of the different sensitivities in each algorithm the artificial effects cannot be completely removed. To minimize the differences due to the algorithm, we take the approach of convolving the averaged AIRS profiles to the MOPITT retrievals for the comparison purposes. We could have, just as easily, convolved the averaged MOPITT profiles to the AIRS retrievals using the AIRS averaging kernels. The fourth column of Figure 6 shows the comparison of these profiles where the red dashed lines represent the convolved AIRS profiles and the dashed blue lines are the convolved DACOM profiles. AIRS and MOPITT CO, under this condition, agree to approximately 10 ppbv for all vertical levels except for the 15 July case when the CO concentration is elevated because of the transport of the fire emissions in the lower atmosphere. AIRS retrievals using MOPITT a priori failed to capture this elevated CO layer while using AFGL first guess provided good agreement as shown in the second left pane on the top row.

3.3. Global Comparisons With Minimized Differences From the a Priori

[23] Both AIRS and MOPITT CO measurements are limited by the observation sensitivities in certain portions of the atmosphere and the prior CO information introduced in the algorithms is partially retained in the final estimations. The selection of the first guess should be based on a global validation and with a thorough understanding of not only the vertical sensitivity but also the constraints of the retrieval. To illustrate the biases between the two data sets, which are completely caused by the uncertainties in the algorithm, the AIRS and MOPITT zonal averaged CO mixing ratios at 500 hPa are shown in Figure 7. Figure 7 (top) shows the differences using AIRS retrievals based on the AFGL first guess profile and Figure 7 (bottom) shows the results using the MOPITT a priori profile as the first

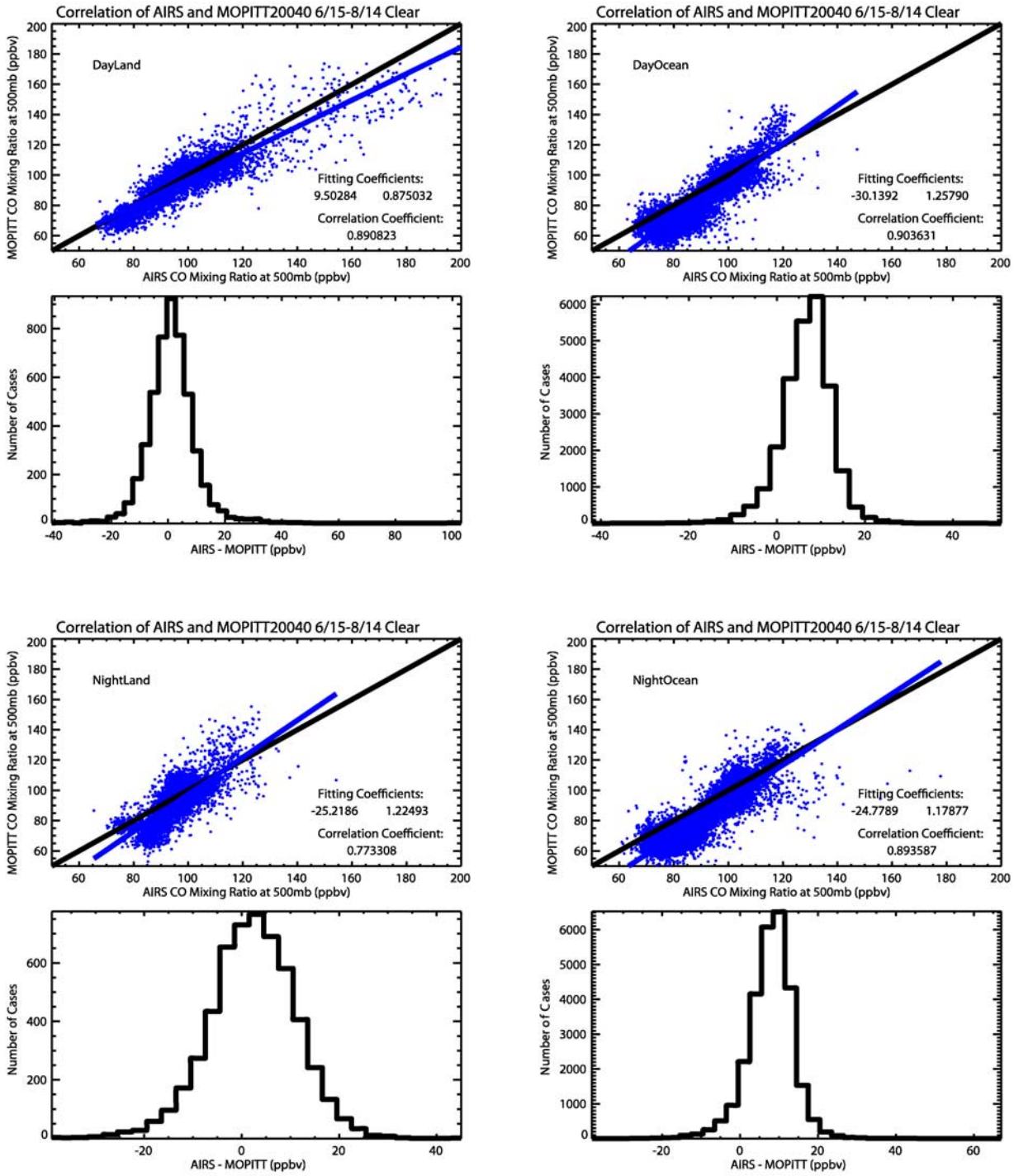

Figure 8. Same as Figure 4 but with AIRS CO retrievals using the MOPITT a priori.

guess for the period of 15 June to 14 August 2004. The scattered data points are the binned AIRS (red) and MOPITT (blue) CO in 1 × 1° latitude/longitude boxes, the solid curves represent the relative zonal averages, and the dashed curves show the data ranges defined by the standard deviations.

[24] AIRS retrievals using the AFGL first guess capture the elevated CO values also seen by MOPITT in the latitude bands in the Northern Hemisphere and the tropics, AIRS estimates higher CO than MOPITT globally. This may be due to a number of factors including that the AFGL profile shows much higher CO values (20–30 ppbv) than the MOPITT a priori in the mid to lower atmosphere. Over clean regions the reason that MOPITT shows much lower CO than AIRS may be due to two factors, one is that much of MOPITT's sensitivity to 500 hPa mixing ratios are from the 700 hPa layer [*Deeter et al.*, 2004], hence MOPITT's retrieval propagates lower CO values from the lower atmo-

sphere to the 500 hPa layers. The other possible reason is that AIRS lacks sensitivity in the lower atmosphere more than MOPITT does. When the MOPITT a priori is used as the first guess in the AIRS retrieval, an average 15–20 ppbv biases between AIRS and MOPITT in the tropics and the Northern hemisphere have been reduced to less than 10 ppbv, resulting in much better agreement between the two data sets. However, as the global agreement between the two data sets is improved, AIRS CO retrievals tend to underestimate elevated CO values in comparison to using the AFGL first guess profile. This reduction in the dynamic range in AIRS' CO retrievals when the first guess profile changed, shown in Figure 7 (bottom), most likely originates from overconstrained damping in the retrieval algorithm. Continued study is underway to completely understand this behavior in the AIRS retrieval algorithm.

[25] The correlation between the two global data sets for the INTEX-A period is recomputed using the MOPITT a priori profile as the AIRS first guess and the results are shown in Figure 8 for daytime land (upper left), daytime ocean (upper right), nighttime land (lower left), and nighttime ocean (lower right), respectively. Although there is very little improvement in the correlation coefficients, the biases as displayed in the histograms are greatly improved. The median values of the biases of 10–20 ppbv over land from the AFGL first guess are removed for both day and nighttime, while over the oceans the biases have been reduced by half. The discrepancy caused by the different correlations between the two sensors for high and low CO, which was shown as a bend in the scatterplots in Figure 4, has also been removed when the same a priori/first guess profile is used by both algorithms. The remaining biases over the oceans can be explained similarly as in the previous section.

4. Conclusions

[26] In this study, we have assessed the quality of the satellite measurements of tropospheric CO by comparing two global products, AIRS and MOPITT, for the period from 15 June to 14 August 2004, during INTEX-A. Using the MOPITT a priori profile as AIRS' first guess provides global improvements to the agreements between CO retrievals from these two instruments. In summary, when the same a priori information is used, both sensors agree very well on the horizontal distributions of CO represented by the high correlation coefficients (0.7–0.98), and they agree on the CO concentrations to within an average of 10–15 ppbv. Over land, the CO variability is higher and the correlations between the two data sets are relatively lower than over ocean, however, there is no evidence of a systematic bias. Over the oceans where the CO concentration is smaller in the lower atmosphere, AIRS tends to overestimate CO concentrations because of a lack of sensitivity.

[27] This comparison study will be extended to include other effects that affect the performance of the satellite retrievals such as the treatments of cloud interferences. Future work will also include the comparison with other similar sensors such as TES on EOS/AURA, IASI on EUMETSAT's METOP, and others. To develop a consistent tropospheric CO data set from different sensors to study the earth climate, it is critical to minimize any disagreements due to the use of different algorithms. Our planned studies include developing a new retrieval algorithm using maximum a posteriori method for AIRS CO so that a better understanding of the instrument sensitivities can be achieved when the same algorithm is used for both sensors.

[28] **Acknowledgments.** The authors wish to thank the INTEX mission scientists, AIRS, and MOPITT teams for making this project possible. This work was funded by NASA grants NNG04GN42G and NNG06GB04G. The authors also wish to thank UMBC colleagues Larrabee Strow, Lynn Sparling, and Alan Chu for many science discussions related to this study and their generosity to share computer resources.

References

Anderson, G., S. Clough, F. Kneizys, J. Chetwynd, and E. Shettel (1986), AFGL atmospheric constituent profiles (0–120 km), *Tech. Rep. AFGL-TR-86-0110*, Air Force Geophys. Lab. (OPI), Hanscom Air Force Base, Mass.

Aumann, H. H., et al. (2003), AIRS/AMSU/HSB on the Aqua mission: Design, science objectives, data products and processing systems, *IEEE Trans. Geosci. Remote Sens.*, *41*, 253–264.

Beer, R., T. A. Glavich, and D. M. Rider (2001), Tropospheric Emission Spectrometer for the Earth Observing System AURA satellite, *Appl. Opt.*, *40*, 2356–2367.

Beer, R. (2006), TES on the Aura mission: Scientific objectives, measurements, and analysis overview, *IEEE Trans. Geosci. Remote Sens.*, *44*, 1102–1105.

Bowman, K. W., T. Steck, H. M. Worden, J. Worden, S. Clough, and C. D. Rodgers (2002), Capturing time and vertical variability of tropospheric ozone: A study using TES nadir retrieval, *J. Geophys. Res.*, *107*(D23), 4723, doi:10.1029/2002JD002150.

Clough, S. A., C. P. Rinsland, and P. D. Brown (1995), Retrieval of tropospheric ozone from simulations of nadir spectral radiances as observed from space, *J. Geophys Res.*, *100*, 16,579–16,593.

Comer, M. M. (2006), Improvements and validation of the Atmospheric Infrared Sounder (AIRS) CO physical retrieval, Ph. D. Dissertation, Univ. of Md. Baltimore Co., Baltimore.

Connors, V. S., B. B. Gormsen, S. Nolf, and H. G. Reichle Jr. (1999), Spaceborne observations of the global distribution of carbon monoxide in the middle troposphere during April and October, 1994, *J. Geophys. Res.*, *104*, 21,455–21,470.

Crutzen, P. J., L. E. Heidt, J. P. Krasnec, and W. H. Pollock (1979), Biomass burning as a source of atmospheric gases CO, H_2, N_2O, NO, CH_3Cl and COS, *Nature*, *282*, 253–256.

Deeter, M. N., et al. (2003), Operational carbon monoxide retrieval algorithm and selected results for the MOPITT instrument, *J. Geophys. Res.*, *108*(D14), 4399, doi:10.1029/2002JD003186.

Deeter, M. N., L. K. Emmons, D. P. Edwards, J. C. Gille, and J. R. Drummond (2004), Vertical resolution and information content of CO profiles retrieved by MOPITT, *Geophys. Res. Lett.*, *31*, L15112, doi:10.1029/2004GL020235.

Drummond, J. R. (1989), Novel correlation radiometer: The length modulated radiometer, *Appl. Opt.*, *28*, 2451–2452.

Emmons, L. K., et al. (2004), Validation of Measurements of Pollution in the Troposphere (MOPITT) CO retrievals with aircraft in situ profiles, *J. Geophys. Res.*, *109*, D03309, doi:10.1029/2003JD004101.

Emmons, L. K., G. G. Pfister, D. P. Edwards, J. C. Gille, G. Sachse, D. Blake, S. Wofsy, C. Gerbig, D. Matross, and P. Nédélec (2007), Measurements of Pollution in the Troposphere (MOPITT) validation exercises during summer 2004 field campaigns over North America, *J. Geophys. Res.*, *112*, D12S02, doi:10.1029/2006JD007833.

Fishman, J., and A. E. Balok (1999), Calculation of daily tropospheric ozone residuals using TOMS and empirically improved SBUV measurements: Application to an ozone pollution episode over the eastern United States, *J. Geophys. Res.*, *104*(D23), 30,319–30,340.

Jonquières, I., and A. Marenco (1998), Redistribution by deep convection and long-range transport of CO and CH_4 emissions from the Amazon basin, as observed by the airborne campaign TROPOZ II during the wet season, *J. Geophys. Res.*, *103*(D15), 19,075–19,092.

Logan, J. A. (1999), An analysis of ozonesonde data for the troposphere: Recommendations for testing 3-D models and development of a gridded climatology for tropospheric ozone, *J. Geophys. Res.*, *104*, 16,115–16,149.

Logan, J. A., M. J. Prather, S. C. Wofsy, and M. B. McElroy (1981), Tropospheric chemistry: A global perspective, *J. Geophys. Res.*, *86*, 7210–7254.

Luo, M., R. Beer, D. J. Jacob, J. A. Logan, and C. D. Rodgers (2002), Simulated observation of tropospheric ozone and CO with the Tropo-

spheric Emission Spectrometer (TES) satellite instrument, *J. Geophys. Res.*, *107*(D15), 4270, doi:10.1029/2001JD000804.

McMillan, W. W., C. Barnet, L. Strow, M. Chahine, J. Warner, M. McCourt, P. Novelli, S. Korontzi, E. Maddy, and S. Datta (2005), Daily global maps of carbon monoxide from NASA's Atmospheric Infrared Sounder, *Geophys. Res. Lett.*, *32*, L11801, doi:10.1029/2004GL021821.

Pan, L., J. C. Gille, D. P. Edwards, P. L. Bailey, and C. D. Rodgers (1998), Retrieval of tropospheric carbon monoxide for the MOPITT experiment, *J. Geophys. Res.*, *103*, 32,277–32,290.

Pfister, G., P. G. Hess, L. K. Emmons, J.-F. Lamarque, C. Wiedinmyer, D. P. Edwards, G. Pétron, J. C. Gille, and G. W. Sachse (2005), Quantifying CO emissions from the 2004 Alaskan wildfires using MOPITT CO data, *Geophys. Res. Lett.*, *32*, L11809, doi:10.1029/2005GL022995.

Reichle, H. G., Jr., and V. S. Connors (1999), The mass of CO in the atmosphere during October 1984, April 1994, and October 1994, *J. Atmos. Sci.*, *56*, 307–310.

Reichle, H. G., et al. (1982), Carbon monoxide measurements in the troposphere, *Science*, *218*, 1024–1026.

Rodgers, C. D. (2000), *Inverse Methods for Atmospheric Sounding, Theory and Practice*, World Sci., River Edge, N. J.

Rodgers, C. D., and B. J. Connor (2003), Intercomparison of remote sounding instruments, *J. Geophys. Res.*, *108*(D3), 4116, doi:10.1029/2002JD002299.

Sachse, G. W., G. F. Hill, L. O. Wade, and M. G. Perry (1987), Fast-response, high precision carbon monoxide sensor using a tunable diode laser absorption technique, *J. Geophys. Res.*, *92*, 2071–2081.

Singh, H. B., W. H. Brune, J. H. Crawford, D. J. Jacob, and P. B. Russell (2006), Overview of the summer 2004 Intercontinental Chemical Transport Experiment–North America (INTEX-A), *J. Geophys. Res.*, *111*, D24S01, doi:10.1029/2006JD007905.

Sparling, L. C. (2000), Statistical perspectives on stratospheric transport, *Rev. Geophys.*, *38*, 417–436.

Strow, L., S. Hannon, S. Machado, H. Motteler, and D. Tobin (2003), An overview of the AIRS radiative transfer model, *IEEE Trans. Geosci. Remote Sens.*, *41*, 303–313.

Susskind, J., C. D. Barnet, and J. M. Blaisdell (2003), Retrieval of atmospheric and surface parameters from AIRS/AMSU/HSB data in the presence of clouds, *IEEE Trans. Geosci. Remote Sens.*, *41*, 390–409.

Warner, J. X., J. C. Gille, D. P. Edwards, D. C. Ziskin, M. W. Smith, and P. L. Bailey (2001), Cloud detection and clearing for the EOS Terra satellite Measurement of Pollution in the Troposphere (MOPITT) experiment, *Appl. Opt.*, *40*(8), 1269–1284.

C. D. Barnet, Center for Satellite Applications and Research, National Environmental Satellite, Data and Information Service, NOAA, 5200 Auth Road, Camp Springs, MD 20746, USA.

M. M. Comer and W. W. McMillan, Department of Physics, University of Maryland Baltimore County, 1000 Hilltop Circle, Baltimore, MD 21250, USA.

E. Maddy and W. Wolf, QSS Group, Inc., Lanham, MD 20706, USA.

G. Sachse, NASA Langley Research Center, Hampton, VA 23681, USA.

J. Warner, Joint Center for Earth Systems Technology, University of Maryland Baltimore County, 5523 Research Park, Baltimore, MD 21250, USA. (juying@umbc.edu)